Chemical Science

ROYAL SOCIETY OF CHEMISTRY

EDGE ARTICLE

View Article Online
View Journal | View Issue

Cite this: *Chem. Sci.*, 2022, **13**, 12396

All publication charges for this article have been paid for by the Royal Society of Chemistry

Received 23rd June 2022
Accepted 29th September 2022

DOI: 10.1039/d2sc03524c

rsc.li/chemical-science

Palladium-catalyzed intramolecular enantioselective C(sp^3)–H insertion of donor/donor carbenes†

Wendeng Li,‡[a] He Zhang,‡[a] Kai Chen,[b] Huanfeng Jiang,[a] Jianwei Sun[c] and Shifa Zhu *[a]

Herein, the first palladium-catalyzed intramolecular enantioselective C(sp^3)–H insertion reaction of donor–donor carbenes has been successfully achieved. This facile protocol enables the rapid construction of a collection of enantioenriched decorated indolines with two contiguous stereocenters in a single step. Both enynones and diazo compounds are efficient donor–donor carbene precursors for this reaction. By an adjustment of ligands and protecting groups of the substrates, the palladium–carbene intermediates from diazo compounds afford sparse *trans*-indolines with excellent enantioselectivities, while carbenes from enynones deliver *cis*-indolines exclusively. Based on the control reactions and Hammett analysis, a stepwise Mannich-type pathway through a short-lived and compact zwitterionic intermediate is proposed.

The asymmetric C–H insertion of metal carbene is one of the most powerful methods for the construction of chiral molecules through carbon–carbon bond formation.[1,2] In the past several decades, many transition metal complexes, especially dirhodium(II) complexes,[2,3] have emerged as effective catalysts for the enantioselective carbene C–H insertion reactions.

Palladium is versatile and indispensable in the formation of C–C and C–heteroatom bonds in cross-coupling chemistry.[4] Palladium-catalyzed carbene transfer reactions, especially cross-couplings *via* the migratory insertion process,[5,6] have been extensively investigated in the past two decades. However, palladium catalyzed carbene-involving asymmetric transformations are still in their infant stage.[7] Taking C–H bond insertion as an example, there are only very limited examples of asymmetric carbenoid C–H insertion reactions in the presence of a palladium catalyst. In 2015 and 2018, Zhou and coworkers reported palladium-catalyzed asymmetric formal carbene insertion into C(sp^2)–H of electron-rich indole and pyrrole derivatives through a Friedel-Crafts-like process with axially chiral bipyridine ligands using aryl diazoesters as the carbene precursor.[7e,h] In 2016, Solé and Fernández reported the first palladium-catalyzed non-asymmetric carbene insertion into an intramolecular C(sp^3)–H bond using diazocarbonyl compounds.[8] It was found that the reaction could be catalyzed by both Pd(0) and Pd(II) (Scheme 1a). DFT calculations revealed that palladium carbene-involving C(sp^3)–H insertion reactions had quite different reaction mechanisms from the related Rh(II)- and Cu-catalyzed reactions.[9] Most notably, the mechanisms of Pd-catalytic systems were affected by the metal valence and substrate structures. For example, Pd(0) and Pd(II) have totally different mechanisms.[8,10] To the best of our knowledge, the palladium-catalyzed enantioselective carbene insertion of C(sp^3)–H bonds still remains unknown. This is probably due to the unique mechanism of palladium carbene chemistry.

Donor-type metal carbenes (donor carbene and donor–donor carbene),[11] owing to the presence of a donor-substituent for stabilization of the carbene carbon center, are typically less

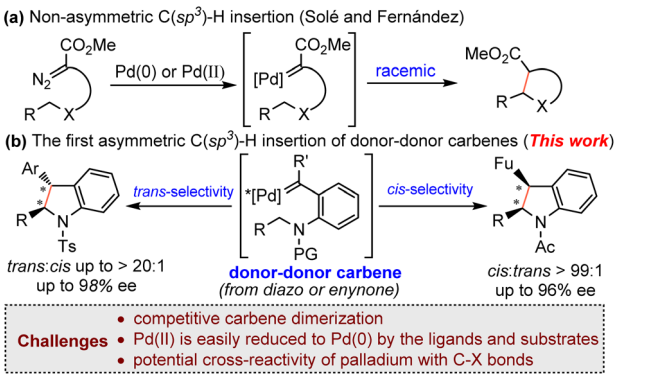

Scheme 1 Pd-catalyzed carbene insertion of a C–H bond.

[a]*Key Lab of Functional Molecular Engineering of Guangdong Province, School of Chemistry and Chemical Engineering, South China University of Technology, Guangzhou, 510640, P. R. China. E-mail: zhusf@scut.edu.cn*

[b]*College of Chemistry and Chemical Engineering, Central South University, Changsha, 410083, P. R. China*

[c]*Department of Chemistry, The Hong Kong University of Science and Technology, Clear Water Bay, Kowloon, Hong Kong SAR, P. R. China*

† Electronic supplementary information (ESI) available. CCDC 2142261, 1908561 and 2142262. For ESI and crystallographic data in CIF or other electronic format see https://doi.org/10.1039/d2sc03524c

‡ These authors contributed equally to this work.

reactive (compared with acceptor-type metal carbenes) and have attracted increasing attention. Recently, Shaw's group[12] and our group[13] have demonstrated the utility of donor-type carbenes in an intramolecular asymmetric C(sp^3)–H insertion reaction in the presence of rhodium and ruthenium catalysts, and diazo compounds, enynones and azaenynes could be used as carbene precursors. As part of our continuing efforts to develop asymmetric carbene transformations,[13,14] along with the unique nature of palladium carbene chemistry, we speculate that the less reactive donor-type carbene intermediate might provide a good opportunity to realize the palladium-catalyzed enantioselective insertion of a C(sp^3)–H bond. However, there are several challenging issues associated with this project: (1) donor-type carbenes are known to easily undergo undesired intermolecular dimerization, resulting in the formation of carbene dimers;[11b] (2) Pd(II) is easily reduced to Pd(0) by the ligands or substrates,[4b,15] which will bring additional complexities in controlling the enantioselectivity; (3) the potential cross-reactivity of palladium with the C–X bond of the reaction components will make the reaction more complicated.[5b] Herein, we report a Pd(II)-catalyzed asymmetric donor–donor carbene insertion into the C(sp^3)–H bond using diazo compounds and enynones (Scheme 1b). This reaction represents the first example of palladium-catalyzed enantioselective C(sp^3)–H bond insertion of donor-type carbenes. Both the diastereo- and enantioselectivity could be well-controlled by tuning the catalytic system.

At the beginning of this investigation, diazo compound **1a** tethered to *N*-benzyltosylamide was chosen as the model substrate to screen the asymmetric intramolecular C(sp^3)–H insertion reaction conditions. As shown in Table 1, different chiral PyBox ligands **L1–L4** were initially tested in the presence of $Pd(PhCN)_2Cl_2$ as the catalyst precursor with $NaBAr^F$ as an additive in toluene (Table 1, entries 1–4). However, the reactions afforded the *cis*-indoline **2a** as the major product with low enantioselectivity. Subsequently, electron-rich axially chiral 2,2′-bipyridines **L5–L7** were then evaluated, which were proven to be effective ligands in promoting the asymmetric C(sp^2)–H functionalization of indoles and pyrroles in Zhou's system.[7e,h] Surprisingly, rare *trans*-indoline[16] **2a** (*trans*/*cis* = 1.2 : 1) could be observed as a slightly dominant product with 93% ee when employing **L6** as a ligand (entry 6). The *cis*/*trans*-selectivity reversal under this reaction condition may arise from the interference of the Ts group with chiral cavity. With a smaller or larger dihedral angle upon chelation with palladium, **L5** or **L7** delivered *trans*-indoline with diminished enantioselectivity (entry 5 and entry 7). Therefore, we chose **L6** as the ligand for further investigation of *trans*-indoline. The reaction was conducted in $CHCl_3$ with poor *trans*-selectivity and enantioselectivity (entry 8). Slightly better *trans*-selectivity was observed in DCE but the enantioselectivity decreased to 88% (entry 9). Solvent screening revealed that $PhCF_3$ was optimal with a moderate *trans*-selectivity (*trans*/*cis* = 1.6 : 1) and a maintained enantioselectivity of 93% ee (entry 10). In addition, the nature of the palladium sources had great impact on the reactivity and selectivity. When using $PdCl_2$, the reaction proceeded to afford the *trans*-indoline **2a** in 46% yield with a 1.7 : 1 *trans*/*cis* ratio and 85% ee (entry 11). $PdCl_2$(cod), containing a 1,5-cyclooctadiene ligand, exhibited a moderate enantioselectivity of 79% ee (entry 12). $Pd(PPh_3)_2Cl_2$, which had more electron-rich triphenylphosphine ligands, strongly eroded the reactivity and enantioselectivity, with only 17% yield and 6% ee (entry 13). To our delight, excellent *trans*-selectivity (*trans*/*cis* = 5.2 : 1) and enantioselectivity (95% ee) were obtained when $Pd(CH_3CN)_2Cl_2$ was used (entry 14). The chloride abstraction additive $NaBAr^F$ was proven necessary for enantioselective control as the ee value dropped dramatically to 4% without $NaBAr^F$ (entry 15). Moreover, palladium(0) complexes were almost ineffective in catalyzing this reaction (see the ESI for details†). In the optimal combination system with $Pd(CH_3CN)_2Cl_2$ and $PhCF_3$, the same type of ligands **L5** and **L7** were retested. **L5** exhibited similar results to **L6** but with a slight improvement of *trans*-selectivity (*trans*/*cis* = 7.3 : 1) and enantioselectivity (95% ee) (entry 16), while **L7** presented slightly decreased selectivities (*trans*/*cis* = 2.8 : 1, 91% ee) (entry 17).

Having identified the optimal reaction conditions (Table 1, entry 14 and entry 16), we then turned our attention to investigate

Table 1 Optimization of the reaction conditions[a]

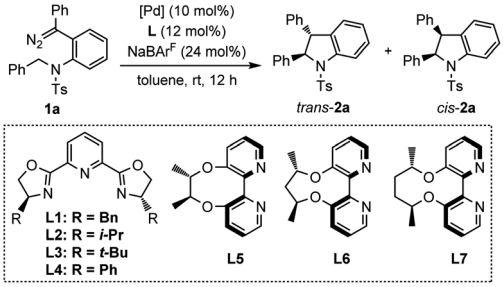

Entry	Catalyst	L	2a yield	2a *trans* : *cis*	ee (*trans*)	ee (*cis*)
1	$Pd(PhCN)_2Cl_2$	**L1**	66%	1 : 15.7	2%	10%
2	$Pd(PhCN)_2Cl_2$	**L2**	44%	1 : 7.3	1%	2%
3	$Pd(PhCN)_2Cl_2$	**L3**	58%	1 : 7.3	15%	4%
4	$Pd(PhCN)_2Cl_2$	**L4**	67%	1 : 9.0	3%	11%
5	$Pd(PhCN)_2Cl_2$	**L5**	54%	1 : 5.7	28%	0%
6	$Pd(PhCN)_2Cl_2$	**L6**	66%	1.2 : 1	93%	8%
7	$Pd(PhCN)_2Cl_2$	**L7**	41%	1 : 3.8	63%	7%
8[b]	$Pd(PhCN)_2Cl_2$	**L6**	69%	1 : 11.5	5%	20%
9[c]	$Pd(PhCN)_2Cl_2$	**L6**	71%	1.7 : 1	88%	2%
10[d]	$Pd(PhCN)_2Cl_2$	**L6**	63%	1.6 : 1	93%	9%
11[d]	$PdCl_2$	**L6**	46%	1.7 : 1	85%	10%
12[d]	$PdCl_2$(cod)	**L6**	49%	1 : 2.3	79%	44%
13[d]	$Pd(PPh_3)_2Cl_2$	**L6**	17%	1 : 2.7	6%	42%
14[d]	**$Pd(CH_3CN)_2Cl_2$**	**L6**	**73%**	**5.2 : 1**	**94%**	**21%**
15[e]	$Pd(CH_3CN)_2Cl_2$	**L6**	19%	1 : 2.1	4%	2%
16[d]	**$Pd(CH_3CN)_2Cl_2$**	**L5**	**65%**	**7.3 : 1**	**95%**	**12%**
17[d]	$Pd(CH_3CN)_2Cl_2$	**L7**	57%	2.8 : 1	91%	19%

[a] **1a** was prepared *in situ* through the oxidization of the corresponding hydrazone by MnO_2 (8.0 eq.); **1a** (0.1 mmol), [**1a**] = 0.033 M; the yield was the isolated yield; the *dr* value (*trans*/*cis*) was determined by using the ^{1}H NMR spectrum of the crude reaction mixture. The ee values of *trans*-**2a** and *cis*-**2a** were determined by HPLC using a chiral stationary phase. [b] The reaction was conducted in $CHCl_3$. [c] The reaction was conducted in DCE. [d] The reaction was conducted in $PhCF_3$. [e] The reaction was conducted in $PhCF_3$ for four days without $NaBAr^F$.

the substrate scope with different diaryl diazo compounds. As shown in Scheme 2, the substrate scope of this asymmetric C(sp^3)–H insertion reaction was found to be quite general, especially the substrates with *N*-benzyl groups. For example, the benzyl moieties with both electron-rich and electron-deficient aryl groups were compatible, furnishing the desired *trans*-indolines in 42–91% yields with 89–98% ee (**2a–t**). Different substituents, such as MeO, MeS, CF_3O, MeO_2C, vinyl, F, Cl, Br and even I, could be introduced at different positions of the benzyl moiety. The reaction enantioselectivities were highly robust for the insertion of benzylic C–H, regardless of the electronic or steric properties, with the ee values typically higher than 90%. However, the diastereoselectivities were a little bit more sensitive to the properties of substituents, with the *dr* ranging from 1.7 : 1 to 7.3 : 1. The *N*-alkyl substrate, which represents a more challenging substrate, could also be subjected to the catalytic reaction conditions, affording the desired products **2u–v** in much better diastereoselectivities (15.7 : 1 and 24 : 1 *dr*) but with diminished enantioselectivities (60% and 86% ee). Furthermore, the varying of groups R^2 had a great effect on the reaction performance. When R^2 was aryl, *trans*-indolines with excellent enantioselectivities could be obtained (**2w**, **2x**). However, the alkyl and ester ones (**2y**, **2z**, and **2ad**) were ineffective in this protocol (see the ESI for details†). To further demonstrate the practicality of this methodology, a gram-scale reaction was conducted, delivering the desired product **2a** in 79% yield, slightly lower diastereoselectivity (3.1 : 1 *dr*) and maintained enantioselectivity (94% ee). In addition, the *N*-Ts group of *trans*-indoline **2a** could be easily removed in the Mg/MeOH system in good yield, and both the diastereo- and enantioselectivity remained unchanged.

In addition to diazo compounds, this palladium-catalytic system could also be extended to an enynone system under modified conditions (see the ESI for more details†). Unlike the above diazo-based system catalyzed by $Pd(CH_3CN)_2Cl_2$/bipyridine, in which *trans*-indolines were obtained, the enynone-based system enabled by $Pd(PhCN)_2Cl_2$/PyBox afforded the corresponding indolines **4** with the *cis*-isomers dominating. As shown in Scheme 3, enynones with different substituted benzylacetamide side chains were subjected to the standard conditions, leading to the desired indolines **4a–f** in 76–85% yields with 80–95% ee. The reactions were a little sensitive to the electronic properties of the substituted group R^1. The electron-rich benzyl groups gave the products in relatively lower ee (**4c**, 80% ee). However, the electron-deficient benzyl groups furnished the products **4d–f** in better enantioselectivities (91–95% ee). Furthermore, this system could be extended to *N*-benzylic enynones with different R^2 groups, delivering the desired products **4g–h** in 63–85% yield and 92–96% ee. However, in the case of *N*-alkyl enynones **3i**, only trace oxidation of carbene was observed with no detectable insertion product even at 120 °C (see the ESI for details†). The absolute configuration of the major enantiomer product was determined by single crystal X-ray diffraction of compound **4h**, which showed a *cis*-(2*R*, 3*S*) configuration. It is noted that the indolines **4** were obtained in higher than 99 : 1 *dr* in all cases, possibly due to the favorable π–π interaction between phenyl and furan substituents.

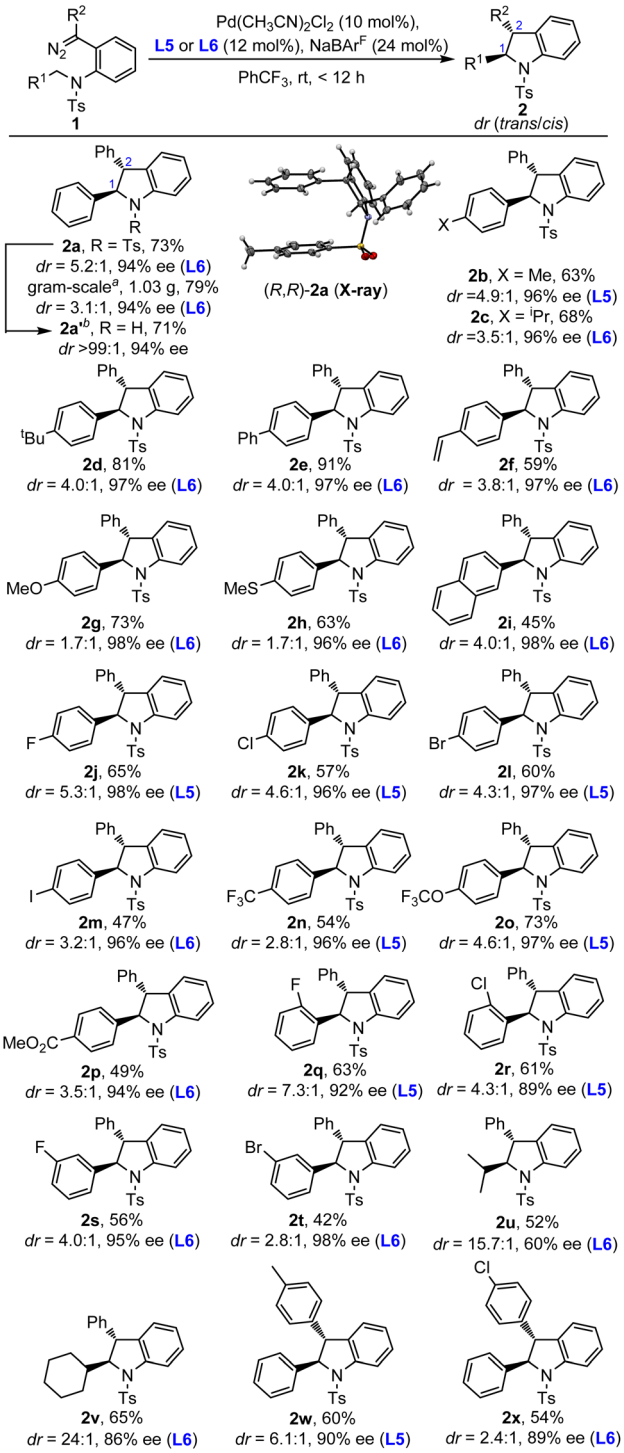

Scheme 2 Substrate scope of diazo compounds. Reaction conditions: **1** was prepared through the oxidization of the hydrazones by MnO_2 (8.0 eq.) and filtered followed by concentration. Then the reactions were run with **1** (0.1 mmol, 0.033 M), $Pd(CH_3CN)_2Cl_2$ (10 mol%), **L5** or **L6** (12 mol%) and $NaBAr^F$ (24 mol%) in $PhCF_3$ under a N_2 atmosphere for 12 h until completion by TLC. [a]The reaction was run with **1a** (3 mmol, 1.40 g, 0.15 M), $Pd(CH_3CN)_2Cl_2$ (9 mol%), **L6** (10.8 mol%) and $NaBAr^F$ (21.6 mol%) in $PhCF_3$ (15 mL) for 15 h. [b]*trans*-**2a** (0.13 mmol), Mg powder (14.0 eq.), methanol (5 mL), 50 °C, sonicate, 2 h.

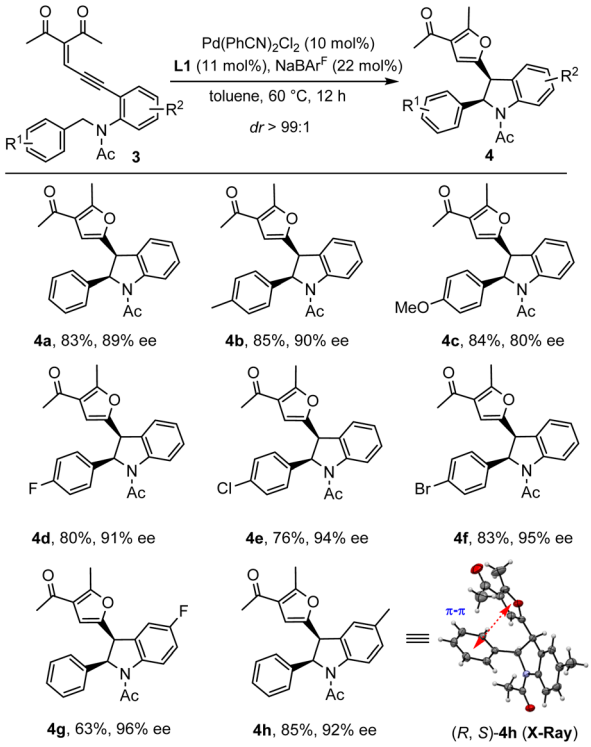

Scheme 3 Substrate scope of enynones. Reaction conditions: **3** (0.2 mmol), $Pd(PhCN)_2Cl_2$ (10 mol%), **L1** (11 mol%) and $NaBAr^F$ (22 mol%) in 1 mL toluene under a N_2 atmosphere at 60 °C for 12 h.

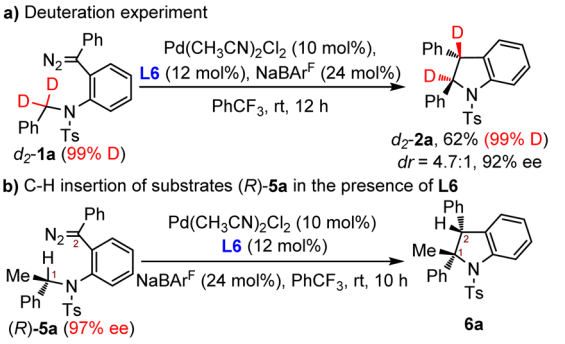

entry	ligand	yield (%)	*cis*:*trans*	ee_{cis} (%)	ee_{trans} (%)
1	*rac*-**L6**	68	94:6	96	97
2	(S_a, *R*, *R*)-**L6**	63	95:5	97	95
3	(R_a, *S*, *S*)-**L6**	36	93:7	92	95
4[a]	(R_a, *S*, *S*)-**L6**	19	68:32	87	98

Scheme 4 Mechanistic investigations. [a]The reaction was conducted at −10 °C.

According to the previous mechanistic studies performed by Solé and Fernández, there are two possible mechanisms for the Pd(II)-catalyzed C(sp^3)–H insertion of an acceptor-type carbene system: (i) the concerted metalation-deprotonation (CMD) process assisted by carbonate or acetate;[8a] (ii) stepwise Mannich-type reaction through a zwitterionic intermediate.[8b] As the reactions in our system were conducted under neutral conditions without the base of carbonate or acetate, the base-assisted CMD mechanism is not likely to be operative. Another stepwise Mannich-type reaction through a zwitterionic intermediate seems more likely. To elucidate the reaction mechanism of our system, several control reactions were conducted. First, when diazo compound d_2-**1a** (99% D) with deuterated methylene was employed as the substrate under the standard reaction conditions, deuterium was completely transferred to the carbene carbon of d_2-**2a** without measurable scrambling of the isotope label (Scheme 4a). Such results indicated that the H-shift occurred intramolecularly without interference from the external solvent or reagents. Second, the kinetic isotope effect (KIE) experiment of monodeuterated diazo compound *d*-**1a** was also performed (see the ESI for details†). The result suggested that the C–H bond cleavage process might not be involved in a rate-determining step. To get more insight into the C(sp^3)–H insertion process, chiral diazo compound (*R*)-**5a** (97% ee) with a tertiary carbon stereocenter was then examined (Scheme 4b). Treatment of (*R*)-**5a** with a palladium catalyst under the standard reaction conditions but with the racemic ligand **L6** provided the *cis*-indoline **6a** as the major product in 68% yield and 94 : 6 *dr* without loss of chiral integrity (Scheme 4b, entry 1). Besides, the chiral ligand (S_a, *R*, *R*)-**L6** produced the stereoretentive indoline **6a** in 63% yield and 95 : 5 *dr* (entry 2). Interestingly, a decreased yield of 36% and enantioselectivity of 92% ee were observed when another stereoisomer of the ligand (R_a, *S*, *S*)-**L6** was used (entry 3), which indicated a mismatch in stereochemical preference between the substrate and Pd-(R_a, *S*, *S*)-**L6** catalyst. What is most unexpected is that the product stereoselectivities further dropped to 87% ee and 68 : 32 *dr* when the catalytic system was cooled down to −10 °C (entry 4). The erosion of chiral integrity during the C–H insertion process indicated that the reaction did not proceed through a concerted process. But the slightly decreased enantioselectivity implied that there might exist a short-lived and compact zwitterionic intermediate after a stereoselective hydride shift which is dominated by the substrate and palladium catalyst.[8b] We envisioned that the chirality erosion of C1 might be caused by the trivial rotation around the C_{aryl}–N bond of the zwitterionic intermediate.

To prove the existence of this zwitterionic intermediate, a Hammett analysis was also conducted with diazo compounds **1** bearing different *para*-substituted benzyl amides. As illustrated in Fig. 1, the small magnitude of the ρ value of −0.29 (R^2 = 0.8338) suggests a slight positive charge buildup at the benzylic carbon atom of the C–H insertion step. Collectively, the stepwise Mannich-type mechanism through a zwitterionic intermediate is likely to be operative for this system.

In light of the opposite diastereoselectivities of C–H insertion behavior for diazo compounds and enynones, we suspected that the difference of *N*-protected groups might lead to the divergence of products. To verify this hypothesis, Ac/Ms/Bn-substituted diazo compound **1aa**/**1ab**/**1ac** was then prepared and subjected to the standard conditions (Scheme 5). As expected, the Ac-substituted diazo **1aa** exclusively produced the *cis*-indoline **2aa** in 54% yield. Ms-substituted diazo **1ab** delivered the *trans*-indoline **2ab** with a 4.3 : 1 *trans* : *cis* ratio similar to that of **2a**. However, as for Bn-substituted diazo **1ac**, only

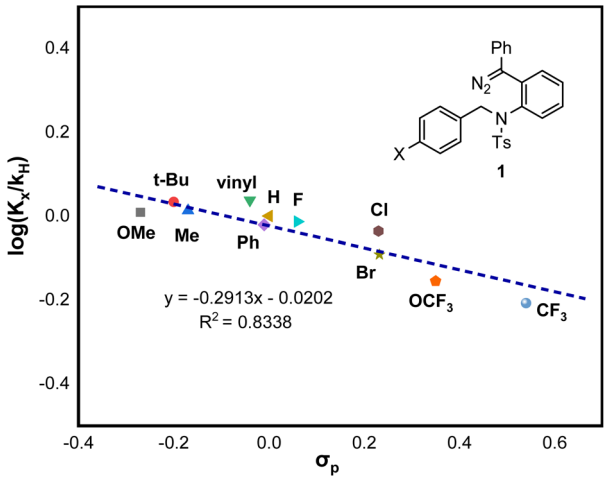

Fig. 1 Hammett analysis.

traces of the C(sp^3)–H insertion product were observed, probably due to the coordination between the amine and palladium complex. These results indicated that the *N*-protected groups of diazo substrates dictated the reaction diastereoselectivities.

Based on the above mechanistic experiments, a plausible mechanism is proposed in Scheme 6. Taking diazo compounds **1a**/**1aa** for example, the reaction starts with the coordination of the diazo and Pd catalyst, followed by extrusion of nitrogen to generate palladium carbene **II**. The intermediate **II** subsequently undergoes a rapid insertion into the C(sp^3)–H bond through a short-lived zwitterionic intermediate **III** to form the products **2a**/**2aa** with the Pd catalyst being regenerated. Based on the structure of ligand **L6** reported by Zhou's group[7e] and the rhodium-diphenylcarbenes reported by Fürstner, Davies and coworkers,[17] two models with different *N*-protected groups are also depicted. The π–π interaction between two phenyl rings could be found in either Ac or Ts-substituted palladium carbene **II**. For *N*-Ac **IIa**, the acetyl group tends to be planar and the rigid structure of acetamide restricts the phenyl on C1 to approaching methyl on acetamide. Combined with the favorable π–π interaction between two phenyl rings, *cis*-indoline is produced exclusively. However, as for *N*-Ts **IIb**, the sulfonyl group is tetrahedral and could rotate to a proper conformation. The introduction of the Ts group would probably change the spatial distribution and thus

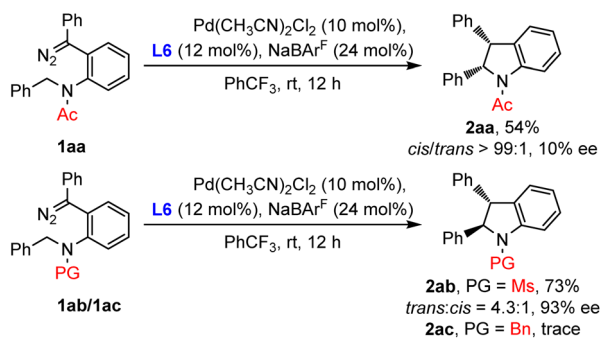

Scheme 5 Investigation into diastereoselectivity.

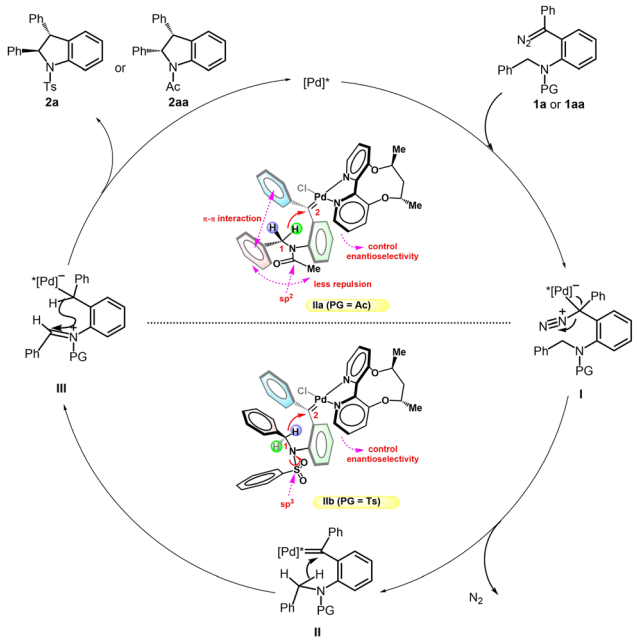

Scheme 6 Plausible reaction mechanism.

reduce steric repulsion or structure strain between the substrate and chiral catalyst. Therefore, a more favorable *trans* configuration would be adopted even though the π–π interaction between two phenyl rings has been weakened. In addition, a high enantioselectivity for *trans*-indoline is attained probably owing to one of the pyridine rings of the axially chiral 2,2′-bipyridine ligand stretching to the reaction center to some extent. It is noteworthy that a stereoretentive ring closure occurs quickly due to the rotation restriction of the iminium ion, and thus the erosion of chirality on C1 by this effect contributes little.

Conclusions

In summary, we have described an effective protocol for the first palladium-catalyzed diastereodivergent asymmetric intramolecular C(sp^3)–H insertion reaction of donor–donor carbenes. Both diazo compounds and enynones can be used as carbene precursors. The reaction shows good functional group tolerance and exhibits excellent diastereo- and enantioselectivity. Opposite configurations of indolines can be accessed by adopting different protecting groups, demonstrating a complementary approach to divergent synthesis. The mechanistic experiments suggest that a stepwise Mannich-type mechanism through a zwitterionic intermediate is more operative for our system. These findings may open new vistas for palladium carbene-involving asymmetric synthesis, especially asymmetric C(sp^3)–H insertions.

Data availability

All the data including experimental procedures, NMR, IR, HRMS, and HPLC spectra and crystallographic data of **2a**, **4h**, (2*R*, 3*S*)-**6a** are recorded in the ESI†.

Author contributions

Conceptualization, funding acquisition, resources and supervision were done or provided by S. Zhu. W. Li and H. Zhang performed all the experiments. K. Chen performed the optimizations of models on reaction diastereoselectivity and enantioselectivity. H. Jiang and J. Sun provided their help with useful discussions and suggestions. W. Li and S. Zhu contributed to the conception of the experiments, discussion of the results and preparation of manuscript.

Conflicts of interest

There are no conflicts to declare.

Acknowledgements

We appreciate financial support from the NSFC (21871096, 22071062, and 22271096) and 111 Project (no. B20003). In addition, Prof. Yonggui Zhou of the Dalian Institute of Chemical Physics (DICP) was acknowledged for his generous supply of the first batch of chiral ligands **L6** and **L7**.

Notes and references

1 For books on asymmetric C–H insertion, see: (*a*) S.-L. You, *Asymmetric Functionalization of C–H Bonds*, RSC, Cambridge, U.K., 2015, pp. 1–66; (*b*) F. Colobert and J. WencelDelord, *C–H Activation for Asymmetric Synthesis*, Wiley-VCH, Weinheim, 2019, pp. 1–49; (*c*) J. Wang, C.-M. Che and M. P. Doyle, *Transition Metal–Catalyzed Carbene Transformations*, Wiley-VCH, Weinheim, 2022, pp. 1–24.

2 For reviews on asymmetric C–H insertion, see: (*a*) H. M. L. Davies and R. E. J. Beckwith, *Chem. Rev.*, 2003, **103**, 2861–2903; (*b*) A. Ford, H. Miel, A. Ring, C. N. Slattery, A. R. Maguire and M. A. McKervey, *Chem. Rev.*, 2015, **115**, 9981–10080; (*c*) Y.-P. Li, Z.-Q. Li and S.-F. Zhu, *Tetrahedron Lett.*, 2018, **59**, 2307–2316; (*d*) H. M. L. Davies and K. Liao, *Nat. Rev. Chem.*, 2019, **3**, 347–360; (*e*) Ł. Woźniak, J.-F. Tan, Q.-H. Nguyen, A. Madron du Vigné, V. Smal, Y.-X. Cao and N. Cramer, *Chem. Rev.*, 2020, **120**, 10516–10543; (*f*) Y. Liu, T. You, H.-X. Wang, Z. Tang, C.-Y. Zhou and C.-M. Che, *Chem. Soc. Rev.*, 2020, **49**, 5310–5358; (*g*) Y. He, Z. Huang, K. Wu, J. Ma, Y.-G. Zhou and Z. Yu, *Chem. Soc. Rev.*, 2022, **51**, 2759–2852; (*h*) B. Hong, L. Shi, L. Li, S. Zhan and Z. Gu, *Green Synth. Catal.*, 2022, **3**, 137–149.

3 For recent selected examples on asymmetric C–H insertion catalyzed by rhodium, see: (*a*) X. Xu, Y. Deng, D. N. Yim, P. Y. Zavalij and M. P. Doyle, *Chem. Sci.*, 2015, **6**, 2196–2201; (*b*) K. Liao, S. Negretti, D. G. Musaev, J. Bacsa and H. M. Davies, *Nature*, 2016, **533**, 230–234; (*c*) K. Liao, T. C. Pickel, V. Boyarskikh, J. Bacsa, D. G. Musaev and H. M. L. Davies, *Nature*, 2017, **551**, 609–613; (*d*) K. Liao, Y. F. Yang, Y. Li, J. N. Sanders, K. N. Houk, D. G. Musaev and H. M. L. Davies, *Nat. Chem.*, 2018, **10**, 1048–1055; (*e*) J. Fu, Z. Ren, J. Bacsa, D. G. Musaev and H. M. L. Davies, *Nature*, 2018, **564**, 395–399; (*f*) W. Liu, Z. Ren, A. T. Bosse, K. Liao, E. L. Goldstein, J. Bacsa, D. G. Musaev, B. M. Stoltz and H. M. L. Davies, *J. Am. Chem. Soc.*, 2018, **140**, 12247–12255; (*g*) Z. J. Garlets, B. D. Wertz, W. Liu, E. A. Voight and H. M. L. Davies, *Chem*, 2020, **6**, 304–313; (*h*) Z. J. Garlets, J. N. Sanders, H. Malik, C. Gampe, K. N. Houk and H. M. L. Davies, *Nat. Catal.*, 2020, **3**, 351–357; (*i*) K. Dong, X. Fan, C. Pei, Y. Zheng, S. Chang, J. Cai, L. Qiu, Z.-X. Yu and X. Xu, *Nat. Commun.*, 2020, **11**, 2363; (*j*) Z. Li, Y. Chen, C. Wang, G. Xu, Y. Shao, X. Zhang, S. Tang and J. Sun, *Angew. Chem., Int. Ed.*, 2021, **60**, 25714–25718.

4 (*a*) J. Tsuji, *Palladium Reagents and Catalysts: New Perspectives for the 21st Century*, Wiley-VCH, Chichester, 2005; (*b*) T. J. Colacot, *New Trends in Cross-Coupling: Theory and Applications*, RSC, Cambridge, U.K., 2015.

5 For reviews on palladium-catalyzed cross-couplings through carbene migratory insertion, see: (*a*) Q. Xiao, Y. Zhang and J. Wang, *Acc. Chem. Res.*, 2013, **46**, 236–247; (*b*) Y. Xia, D. Qiu and J. Wang, *Chem. Rev.*, 2017, **117**, 13810–13889; (*c*) K. Wang and J. Wang, *Synlett*, 2019, **30**, 542–551; (*d*) Y. Xia and J. Wang, *J. Am. Chem. Soc.*, 2020, **142**, 10592–10605.

6 For selected examples on palladium-catalyzed cross-couplings through carbene migratory insertion, see: (*a*) K. L. Greenman, D. S. Carter and D. L. Van Vranken, *Tetrahedron*, 2001, **57**, 5219–5225; (*b*) J. Barluenga, P. Moriel, C. Valdés and F. Aznar, *Angew. Chem., Int. Ed.*, 2007, **46**, 5587–5590; (*c*) R. Kudirka, S. K. Devine, C. S. Adams and D. L. Van Vranken, *Angew. Chem., Int. Ed.*, 2009, **48**, 3677–3680; (*d*) Y. Gao, G. Wu, Q. Zhou and J. Wang, *Angew. Chem., Int. Ed.*, 2018, **57**, 2716–2720; (*e*) Z. Liu, S. Cao, J. Wu, G. Zanoni, P. Sivaguru and X. Bi, *ACS Catal.*, 2020, **10**, 12881–12887; (*f*) Y. Ping, R. Wang, Q. Wang, T. Chang, J. Huo, M. Lei and J. Wang, *J. Am. Chem. Soc.*, 2021, **143**, 9769–9780; (*g*) X. Ning, Y. Chen, F. Hu and Y. Xia, *Org. Lett.*, 2021, **23**, 8348–8352; (*h*) S. Li, M. Li, S.-S. Li and J. Wang, *Chem. Commun.*, 2022, **58**, 399–402.

7 For examples on palladium carbene-involving asymmetric transformations, see: (*a*) A. Khanna, C. Maung, K. R. Johnson, T. T. Luong and D. L. Van Vranken, *Org. Lett.*, 2012, **14**, 3233–3235; (*b*) D. Zhang, H. Qiu, L. Jiang, F. Lv, C. Ma and W. Hu, *Angew. Chem., Int. Ed.*, 2013, **52**, 13356–13360; (*c*) Y. Zhu, X. Liu, S. Dong, Y. Zhou, W. Li, L. Lin and X. Feng, *Angew. Chem., Int. Ed.*, 2014, **53**, 1636–1640; (*d*) X.-L. Xie, S.-F. Zhu, J.-X. Guo, Y. Cai and Q.-L. Zhou, *Angew. Chem., Int. Ed.*, 2014, **53**, 2978–2981; (*e*) X. Gao, B. Wu, W.-X. Huang, M.-W. Chen and Y.-G. Zhou, *Angew. Chem., Int. Ed.*, 2015, **54**, 11956–11960; (*f*) J. Feng, B. Li, Y. He and Z. Gu, *Angew. Chem., Int. Ed.*, 2016, **55**, 2186–2190; (*g*) V. Arredondo, S. C. Hiew, E. S. Gutman, I. D. U. A. Premachandra and D. L. Van Vranken, *Angew. Chem., Int. Ed.*, 2017, **56**, 4156–4159; (*h*) H.-Q. Shen, C. Liu, J. Zhou and Y.-G. Zhou, *Org. Chem. Front.*, 2018, **5**, 611–614; (*i*) H.-Q. Shen, H.-P. Xie, L. Sun and Y.-G. Zhou, *Organometallics*, 2019, **38**, 3902–3905; (*j*) J. Huo, K. Zhong, Y. Xue, M. Lyu, Y. Ping, Z. Liu, Y. Lan and J. Wang, *J. Am.*

Chem. Soc., 2021, **143**, 12968–12973; (*k*) J. Huo, K. Zhong, Y. Xue, M. Lyu, Y. Ping, W. Ouyang, Z. Liu, Y. Lan and J. Wang, *Chem. - Eur. J.*, 2022, **28**, e202200191; (*l*) B. Yang, B. K. Cao, G. Zhao, J. Yang and J. Zhang, *J. Am. Chem. Soc.*, 2022, **144**, 15468–15474.

8 (*a*) D. Solé, F. Mariani, M. L. Bennasar and I. Fernández, *Angew. Chem., Int. Ed.*, 2016, **55**, 6467–6470; (*b*) D. Solé, F. Pérez-Janer, M. L. Bennasar and I. Fernández, *Eur. J. Org. Chem.*, 2018, **2018**, 4446–4455.

9 E. Nakamura, N. Yoshikai and M. Yamanaka, *J. Am. Chem. Soc.*, 2002, **124**, 7181–7192.

10 (*a*) Y. Zhang and J. Wang, *Eur. J. Org. Chem.*, 2011, 1015–1026; (*b*) D. G. Musaev, T. M. Figg and A. L. Kaledin, *Chem. Soc. Rev.*, 2014, **43**, 5009–5031.

11 (*a*) M. Mato, C. García-Morales and A. M. Echavarren, *ChemCatChem*, 2018, **11**, 53–72; (*b*) D. Zhu, L. Chen, H. Fan, Q. Yao and S. Zhu, *Chem. Soc. Rev.*, 2020, **49**, 908–950; (*c*) B. D. Bergstrom, L. A. Nickerson, J. T. Shaw and L. W. Souza, *Angew. Chem., Int. Ed.*, 2021, **60**, 6864–6878; (*d*) R. Vicente, *Chem. Rev.*, 2021, **121**, 162–226; (*e*) M. Mato, A. Franchino, C. García-Morales and A. M. Echavarren, *Chem. Rev.*, 2021, **121**, 8613–8684.

12 (*a*) C. Soldi, K. N. Lamb, R. A. Squitieri, M. González-López, M. J. Di Maso and J. T. Shaw, *J. Am. Chem. Soc.*, 2014, **136**, 15142–15145; (*b*) K. N. Lamb, R. A. Squitieri, S. R. Chintala, A. J. Kwong, E. I. Balmond, C. Soldi, O. Dmitrenko, M. Castiñeira Reis, R. Chung, J. B. Addison, J. C. Fettinger, J. E. Hein, D. J. Tantillo, J. M. Fox and J. T. Shaw, *Chem. - Eur. J.*, 2017, **23**, 11843–11855; (*c*) L. W. Souza, R. A. Squitieri, C. A. Dimirjian, B. M. Hodur, L. A. Nickerson, C. N. Penrod, J. Cordova, J. C. Fettinger and J. T. Shaw, *Angew. Chem., Int. Ed.*, 2018, **57**, 15213–15216; (*d*) L. A. Nickerson, B. D. Bergstrom, M. Gao, Y. S. Shiue, C. J. Laconsay, M. R. Culberson, W. A. Knauss, J. C. Fettinger, D. J. Tantillo and J. T. Shaw, *Chem. Sci.*, 2020, **11**, 494–498; (*e*) S. N. Dishman, C. J. Laconsay, J. C. Fettinger, D. J. Tantillo and J. T. Shaw, *Chem. Sci.*, 2022, **13**, 1030–1036; (*f*) B. D. Bergstrom, A. T. Merrill, J. C. Fettinger, D. J. Tantillo and J. T. Shaw, *Angew. Chem., Int. Ed.*, 2022, **61**, e2022030.

13 (*a*) D. Zhu, J. Ma, K. Luo, H. Fu, L. Zhang and S. Zhu, *Angew. Chem., Int. Ed.*, 2016, **55**, 8452–8456; (*b*) D. Zhu, L. Chen, H. Zhang, Z. Ma, H. Jiang and S. Zhu, *Angew. Chem., Int. Ed.*, 2018, **57**, 12405–12409; (*c*) S. Qiu, X. Gao and S. Zhu, *Chem. Sci.*, 2021, **12**, 13730–13736.

14 (*a*) R. Wu, K. Chen, J. Ma, Z.-X. Yu and S. Zhu, *Sci. China: Chem.*, 2020, **63**, 1230–1239; (*b*) Z. Liu, L. Chen, D. Zhu and S. Zhu, *Org. Lett.*, 2021, **23**, 1275–1279; (*c*) R. Wu, J. Lu, T. Cao, J. Ma, K. Chen and S. Zhu, *J. Am. Chem. Soc.*, 2021, **143**, 14916–14925; (*d*) D. Zhu, T. Cao, K. Chen and S. Zhu, *Chem. Sci.*, 2022, **13**, 1992–2000.

15 Y. V. Tomilov, V. A. Dokitchev, U. M. Dzhemilev and O. M. Nefedov, *Russ. Chem. Rev.*, 1993, **62**, 799–838.

16 M. Santi, S. T. R. Müller, A. A. Folgueiras-Amador, A. Uttry, P. Hellier and T. Wirth, *Eur. J. Org. Chem.*, 2017, **2017**, 1889–1893.

17 (*a*) C. Werlé, R. Goddard, P. Philipps, C. Farès and A. Fürstner, *J. Am. Chem. Soc.*, 2016, **138**, 3797–3805; (*b*) M. Lee, Z. Ren, D. G. Musaev and H. M. L. Davies, *ACS Catal.*, 2020, **10**, 6240–6247.